$$V(r)=\frac{-V_0}{1+\exp[(r-r_0)/a]} \quad (2)$$

Where a, is the diffuseness parameter.
In general the intrinsic degree of freedom ξ has a finite spin. We therefore expand the coupling Hamiltonian in multipoles as [6],

$$V_{coup}(r,\xi)=\sum_{\lambda>0} f_\lambda(r) Y_\lambda(\hat{r})\cdot T_\lambda(\xi) \quad (3)$$

Here $Y_\lambda(\hat{r})$ are the spherical harmonics and $T_\lambda(\xi)$ are spherical tensors constructed from the intrinsic coordinate. The dot indicates a scalar product. The sum is taken over all except for λ = 0, which is already included in the bare potential, $V(r)$. For a fixed total angular momentum J and its z-component M, the expansion basis for the wave function in Eq. (2) are defined as [5],

$$\langle \hat{r},\xi|(\alpha l I)JM\rangle=\sum_{m_l,m_I}\langle l m_l\, I\, m_I|JM\rangle Y_{lm_l}(\hat{r})\varphi_{\alpha I m_I}(\xi) \quad (4)$$

Where l and I are the orbital and the intrinsic angular momenta, respectively $\varphi_{\alpha I m_I}(\xi)$ are the wave functions of the intrinsic motion which obey,

$$H_0(\xi)\varphi_{\alpha I m_I}(\xi)=\varepsilon_{\alpha I}\varphi_{\alpha I m_I}(\xi) \quad (5)$$

Here, α denotes any quantum number besides the angular momentum. Expanding the total wave function with the channel wave functions as [5],

$$\psi_J(r,\xi)=\sum_{\alpha,l,I}\frac{u^J_{\alpha l I}(r)}{r}\langle \hat{r},\xi|(\alpha l I)JM\rangle \quad (6)$$

The coupled-channels equations for $u^J_{\alpha l I}(r)$ read [5],

$$\left[-\frac{\hbar^2}{2\mu}\frac{d^2}{dr^2}+\frac{l(l+1)\hbar^2}{2\mu r^2}+V(r)-E+\varepsilon_{\alpha I}\right]u^J_{\alpha l I}(r) + \sum_{\alpha',l',I'}V^J_{\alpha l I;\alpha' l' I'}(r)u^J_{\alpha' l' I'}(r)=0 \quad (7)$$

Where the coupling matrix elements $V^J_{\alpha l I;\alpha' l' I'}(r)$ are given as [7],

$$\begin{aligned}V^J_{\alpha l I;\alpha' l' I'}(r)&=\langle(\alpha l I)JM|V_{coup}(r,\xi)|(\alpha' l' I')JM\rangle,\\ &=\sum_\lambda(-1)^{I-I'+l'+J}f_\lambda(r)\langle l\|Y_\lambda\|l'\rangle\langle\alpha I\|T_\lambda\|\alpha' I'\rangle \quad (8)\\ &\times\sqrt{(2l+1)(2I+1)}\begin{Bmatrix}I' & l' & J\\ l & I & \lambda\end{Bmatrix}.\end{aligned}$$

Notice that these matrix elements are independent of M. For the sake of simplicity of the notation, in the following let us introduce a simplified notation, n = {α, l, I}, and suppress the index J. The coupled-channels Eq. (7) then reads [5],

$$\left[-\frac{\hbar^2}{2\mu}\frac{d^2}{dr^2}+\frac{l(l+1)\hbar^2}{2\mu r^2}+V(r)-E+\varepsilon_n\right]u_n(r) + \sum_{\alpha',l',I'}V_{nn'}(r)u_{n'}(r)=0 \quad (9)$$

These coupled-channels equations are solved with the incoming wave boundary conditions of [5],

$$\begin{aligned}u_n(r)&\approx\sqrt{\frac{k_{n_i}}{k_n(r)}}\Im^J_{nn_i}\exp\left(-i\int_{r_{abs}}^{r}k_n(r')dr'\right) \qquad r\le r_{abs}, \quad (10)\\ &=H^{(-)}_{l n}(k_n r)\delta_{n,n_i}-\sqrt{\frac{k_{n_i}}{k_n}}S^J_{nn_i}H^{(+)}_{l n}(k_n r) \qquad r\to\infty\end{aligned}$$

Where ni denotes the entrance channel. The local wave number kn (r) is defined by,

$$k_n(r)=\sqrt{\frac{2\mu}{\hbar^2}\left(E-\varepsilon_n-\frac{l_n(l_n+1)}{2\mu r^2}-V(r)\right)} \quad (11)$$

Where $k_n=k_n(r=\infty)=\sqrt{2\mu(E-\varepsilon_n)/\hbar^2}$ .Once the transmission coefficients $\Im^J_{nn_i}$ are obtained, the inclusive penetrability of the Coulomb potential barrier is given by,

$$P_J(E)=\sum_n\left|\Im^J_{nn_i}\right|^2 \quad (12)$$

The fusion cross section is then given by [5],

$$\sigma_{fus}(E)=\frac{\pi}{k^2}\sum_J(2J+1)P_J(E) \quad (13)$$

The fusion barrier distribution is given by [8],

$$D_f(E)=\frac{d^2(E\sigma_{fus})}{dE^2}=\pi R_b^2\left[-\frac{d}{dE}\left(\frac{1}{1+\exp\left[2\pi\frac{E-V_b}{\hbar\omega}\right]}\right)\right] \quad (14)$$

3. Fusion Barrier Distributions

Over recent years precision measurements of “experimental fusion barrier distributions” have led to significant insights into how the collective modes (rotational and vibrational) of the target and projectile influence the dynamics of a nuclear reaction. The simple idea behind these measurements is that since the classical fusion cross σ_{fus} (zero below the Coulomb barrier) is given above the barrier by [5],

$$E\sigma_{fus}=\pi R^2(E-B) \quad (15)$$

Where B and R are the Coulomb barrier heights and radius, and E is the incident center of mass energy. Then the second derivative $d^2(E\sigma_{fus})/dE^2$ is simply a delta function of area πR^2 located at the energy E = B. quantum tunneling merely smooth out this function into a symmetric peak with a width of around 2-3 (MeV), but if a range of barriers wider than that value is present in a given reaction then their “distribution” can be readily deduced from [5],

$$D_{fus}=d^2(E\sigma_{fus})/dE^2 \quad (14)$$

The second derivative of ($E\sigma_{fus}$) was extracted from the excitation functions using a simple point difference method. It is defined at energy (*E1* + *2E2* + *E3*)/4 as,

$$\frac{d^2(E\sigma_{fus})}{dE^2}=2\left(\frac{(E\sigma_{fus})_3-(E\sigma_{fus})_2}{E_3-E_2}-\frac{(E\sigma_{fus})_2-(E\sigma_{fus})_1}{E_2-E_1}\right)\left(\frac{1}{E_3-E_1}\right) \quad (15)$$

where $(E\sigma_{fus})_i$ are evaluated at energies E_i .
with equal energy increments $\Delta E=(E_2-E_1)=(E_3-E_2)$ this reduces to,

$$\frac{d^2(E\sigma_{fus})}{dE^2}=\left(\frac{(E\sigma_{fus})_3-2(E\sigma_{fus})_2+(E\sigma_{fus})_1}{\Delta E^2}\right) \quad (16)$$

Then the statistical error (δ_c) associated with the second derivative at energy E is approximately given by,

$$\delta_c \cong (E/\Delta E^2)\left[(\delta\sigma_{fus})_1^{\,2} + 4(\delta\sigma_{fus})_2^{\,2} + (\delta\sigma_{fus})_3^{\,2}\right]^{1/2} \qquad (17)$$

where the $(\delta\sigma_{fus})$ are the errors in the cross sections. They have dimensions of cross sections and are not percentage errors. Thus when, as is common, the (σ_{fus}) are measured with a fixed percentage error, (δ_c) is proportional to the value of (σ_{fus}) and increases with increasing energy [9].

4. Results and Discussion

4.1 $^{16}O+^{144}Sm$ System

The coupled-channels calculations of fusion cross section as well as fusion barrier distribution for the heavy ion reaction of $^{16}O+^{144}Sm$ System by including the lowest state of ^{144}Sm, that is, $^-3$ (octupole) (single phonon) and $^-3$ (octupole) (double phonon).

The results of coupled-channels calculations are performed by using the CCFULL code [10] are compared with the experimental data in Fig. 1. Fig. 1(a) and 1(b) shows the fusion cross section and the fusion barrier distribution, respectively. The dotted line represents the calculations without including the coupling effects, i.e., the target and the projectile are assumed to be inert in which the calculations of the fusion cross section underestimate the experimental data at and below the Coulomb barrier. The solid line represents the results of the calculations taking the single phonon state of the octupole excitations into account, where the calculated fusion cross section are in excellent fit with the experimental data below and above the Coulomb barrier. The calculations including the double octupole phonon states in addition to single octupole vibration is shown by dashed line overestimated the experimental data. The woods-Saxon parameters are taken to be, V_0=105.1 MeV, r_0=1.06 fm., a_0=0.75 fm. The fusion barrier distribution are extracted from the experimental data and from the theoretical calculations of the fusion cross section by using the simple three point difference method in which Matlab code was written to do these calculations. Our calculations agrees very well with the previous work (see. Refs. [9,11,12]).

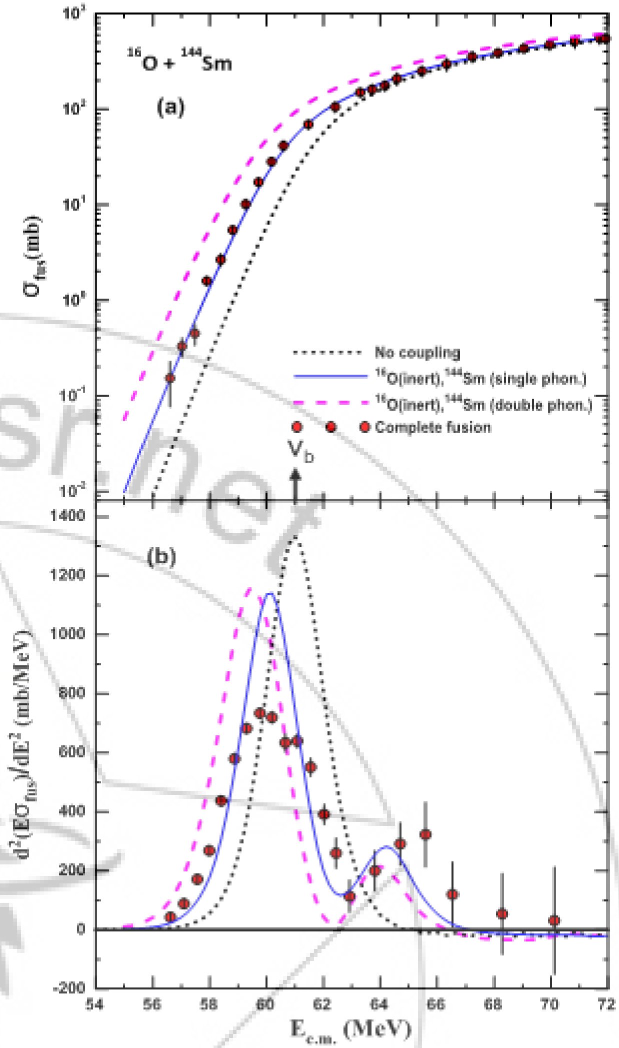

Figure 1: Comparison of coupled-channels calculations with the experimental data for $^{16}O+^{144}Sm$ for (a) the fusion cross and (b) the fusion barrier distribution. The dotted line is the result without coupling. The coupled-channels calculations which take into account the coupling to single quadrupole and octupole excitations in ^{144}Sm is given by solid line. The dashed line is obtained by including the coupling to double quadrupole phonon excitations in addition to single octupole state in target nucleus. Experimental data are taken from Leigh et al. [9].

4.2 $^{16}O+^{154}Sm$ System

The calculation of the total fusion cross fusion and the fusion barrier distribution are presented in Fig.2 (a) and Fig.2(b). Since ^{154}sm is a well deformed nuclei the code defus[10] are employed with deformation parameters β_2=0.322 and β_4=0.05 to account for the rotational deformation for ^{154}sm, while the projectile is kept inert. The dotted line in Fig. 2 (a) and (b) represents the calculations without including coupling, i.e., both projectile and target are inert we can see from the figure that without coupling the calculation of the fusion cross section underestimate the experimental data around and below the Coulomb barrier and the calculations of the fusion barrier distribution centered around the Coulomb barrier are unable to reproduce the experimental data. The solid line represents the calculations by considering the rotation in the target nucleus with deformation parameters mentioned above which agrees very well with the experimental data and enhance the calculations of the fusion cross section around and below the Coulomb barrier. The woods-Saxons parameters are taken to be V_0=165 MeV, r_0=0.95 fm, a_0=1.05 fm.

5. Conclusions

The effect of coupled channels are investigated for the systems $^{16}O+^{144}Sm$ and $^{16}O+^{154}Sm$ and we concluded that the coupling of the octupole state in ^{144}Sm target nucleus are very essential and leads to enhance the total fusion cross section calculations and also leads to reasonable agreement with the experimental data for the fusion barrier distributions.

It has been found that the coupling of low lying vibrational states with the relative motion of interacting nuclei enhances the sub-barrier fusion cross-section to large extent as compared with the one dimensional barrier penetration model calculations. Further, the extent of enhancement of the sub-barrier fusion cross section has been found to be very sensitive to the deformation parameter and the energy of the states included in the analysis. This work can be extended to study heavier nuclei and also to study the effect of the breakup channel for halo nuclei.

6. Acknowledgments

The authors would like to acknowledge the financial support from the department of physics, college of education for pure sciences, University of Babylon.

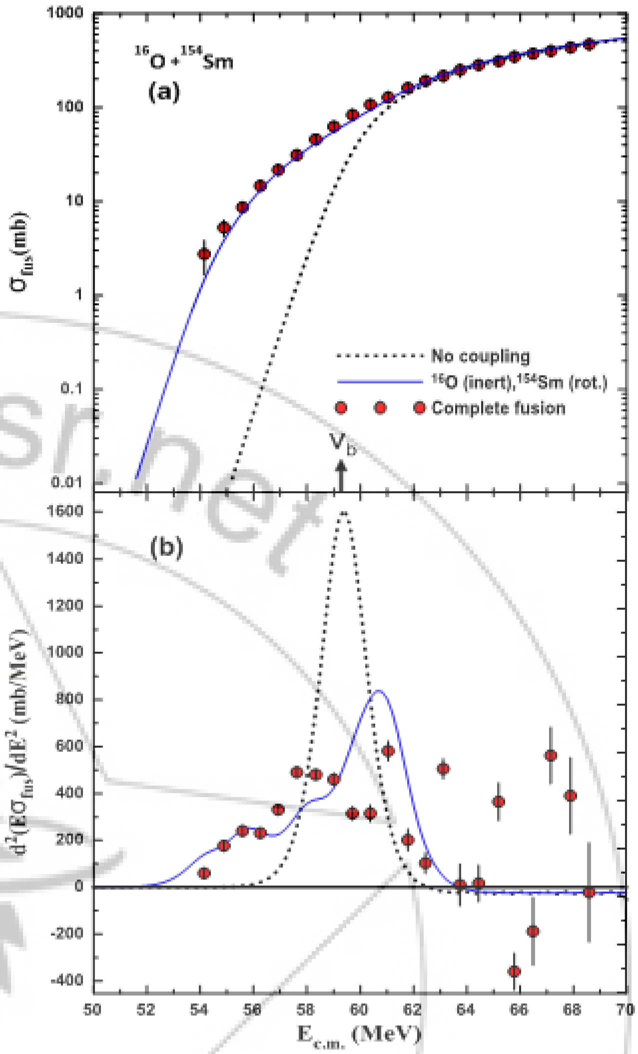

Figure 2: Comparison of coupled-channels calculations with the experimental data for $^{16}O+^{154}Sm$ for (a) the fusion cross and (b) the fusion barrier distribution. The dotted line is the result without coupling. The coupled-channels calculations which take into account the rotational coupling for the target nucleus ^{154}Sm is given by solid line. Experimental data are taken from Leigh et al.[9].

References

[1] S. Kalkal, S. Mandal, N. Madhavan, A. Jhingan, E. Prasad, R. Sandal, J. Gehlot, S.Verma, R. Garg, S. Goyal, M. Saxena, S. Nath, B. Behera, S. Kumar, U. D. Pramanik, D. Siwal, G. Mohanto, H. J. Wollersheim, A. K. Sinha and R. Singh, "Fusion and transfer reactions around the Coulomb barrier for 28Si+90,94Zr systems" , Journal of Phyiscs: Conference Series 312, pp. 082027-082033, 2011.

[2] A. B. Balantekin and N. Takigawa, "Quantum tunneling in nuclear fusion", Review of Modern Physics, 70, pp. 77-100, 1998.

[3] N. Rowley, "Geiger-Marsden experiments: 100 years on", Journal of Physics, International Conference on Nucleus-Nucleus Collisions (NN2012), Conference Series 381, pp.012086-012092, 2012.

[4] S.V. S. Sastry and S. Santra, "Structure information from fusion barriers", Pramana – Journal of Physics, Vol. 54, No.6., pp. 813–826, 2000.

[5] K. Hagino and N. Takigawa, “Subbarrier Fusion Reactions and Many-Particle Quantum Tunneling”, Progress of Theoretical Physics, Volume 128, Issue 6, pp. 1001-1060, 2012.
[6] F. M. Zamrun, “ Coupled-channels analyses for heavy-ion fusion reaction and quasi-elastic scattering around the Coulomb barrier”, PhD thesis, Beijing University, 2008.
[7] A. R. Edmonds A.R. 1960, Angular Momentum in Quantum Mechanics, Princeton University Press, Princeton, New Jersey, 1960.
[8] L. F. Canto, P.R.S. Gomes, R. Donangelo, M.S. Hussein, “Fusion and breakup of weakly bound nuclei”, Physics Reports, pp.1-111, 2006.
[9] J. R. Leigh, M. Dasgupta, D. J. Hinde, J. C. Mein, C. R. Morton, R. C. Lemmon, J. P. Lestone, J. O. Newton, H. Timmers, J. X. Wei and N. Rowley, “Barrier distributions from the fusion of oxygen ions with $^{144,148,154}Sm$ and ^{186}W”, Physical Review C 52, pp. 3151-3166, 1995.
[10] K. Hagino, N. Rowley, A.T. Kruppa, “A program for coupled-channel calculations with all order couplings for heavy-ion fusion reactions”, Computer Physics Communications, 123, pp.143–152, 1999.
[11] C. R. Morton, M. Dasgupta, D. J. Hinde, J. R. Leigh, R. C. Lemmon, J. P. Lestone, J. C. Mein, J. O. Newton, H. Timmers, N. Rowley, and A. T. Kruppa, “Clear signatures of specific inelastic and transfer channels in the distribution of fusion barriers”, Physical Review Letters, 72, pp. 4074-4077, 1994.
[12] U. Jahnke, H. H. Rossner, D. Hilscher, and E. Holub, “Global Increase of Near- and Below-Barrier Fusion for Heavier Systems”, Physical Review Letters, 48, pp. 17-20, 1982.

Author Profile

Fouad A. Majeed born in Babylon (1974). He is assistant professor at University of Babylon. His fields of expertise are study of nuclear reactions and nuclear structure. He has received awards as visiting scientist from The Abdus Salam (ICTP) and post-doctoral fellow from TWAS-CNPq. He obtained his B.Sc. from Al-Mustansiriyah University 1997, his M.Sc. (2000) and Ph.D. (2005) from Al-Nahrain University.